Civil Engineering

Accurate numerical analysis of large deflections in axially deformable prismatic and non-prismatic cantilever beams and columns

http://dx.doi.org/10.1590/0370-44672025790050

Aleff Gonçalves Quintino[1,2]
https://orcid.org/0000-0002-5456-0332
Marcelo Greco[1,3]
https://orcid.org/0000-0001-5500-0225

[1]Universidade Federal da Minas Gerais – UFMG,
Escola de Engenharia, Departamento de
Engenharia de Estruturas,
Belo Horizonte - Minas Gerais - Brasil.

E-mails: [2]aleff.quintino@gmail.com,
[3]mgreco@dees.ufmg.br

Abstract

This article presents a numerical analysis of large deflections (elastica) in prismatic and non-prismatic cantilever beams and columns subjected to either concentrated or uniformly distributed loads, accounting for axial deformation. A mathematical model is derived, consisting of three coupled differential equations that govern the position of the member in its deformed configuration. The nonlinear boundary value problem is solved using an accurate numerical procedure based on the Dormand–Prince Runge–Kutta method, combined with the shooting method. Highly accurate tabulated results are presented for various taper ratios (ranging from 0.2 to 1.0) of a rectangular cross-section with linearly varying height, including free-end positions, buckling loads, and post-buckling behavior. Differences in the responses are observed when axial deformation is neglected, particularly in members with predominantly axial loading, varying according to the taper ratio. When axial deformation is neglected, the results show good agreement with available analytical and numerical solutions, demonstrating the accuracy of the proposed approach.

Keywords: large deflections, axial deformation, non-prismatic members, nonlinear differential equations.

1. Introduction

In the development of a formulation based on the Finite Element Method (FEM) for the geometrically nonlinear analysis of framed structures (e.g., beams, columns, rods, robotic arms), shells, and solids, it is essential to compare the obtained results with either an analytical solution or a highly accurate numerical solution derived from the governing mathematical model.

In this context, closed-form analytical solutions of nonlinear Ordinary Differential Equations (ODEs) in terms of elliptic integrals, related to the analysis of large deflections of beams or columns, are available only in special cases, such as: a straight prismatic cantilever beam or column with a concentrated load at the free end (Barten, 1944; Bisshopp and Drucker, 1945; Timoshenko and Gere, 1961, 1972; Mattiasson, 1981); a straight prismatic cantilever beam under two concentrated loads (Frisch-Fay, 1962a); an initially curved (circular) prismatic cantilever beam or column with a concentrated load at the free end (Frisch-Fay, 1962b); a simply supported straight prismatic beam with a moment applied at one end (Seide, 1984); and a simply supported straight prismatic beam subjected to a point load (Conway, 1947; Wang *et al*., 1997).

However, numerical solutions are required for situations involving prismatic members under distributed loads (Hummel and Morton, 1927; Bickley, 1934; Rohde, 1953; Frisch-Fay, 1961; Schmidt and Dadeppo, 1970; Holden, 1972; Rao and Raju, 1977; Wang, 1981, 1987; Rao, B. N. and Rao, G. V., 1988a, 1989; Lee, 2001) and non-prismatic members under point and/or distributed loads (Rao, B. N. and Rao, G. V., 1988b; Baker, 1993; Lee and Oh, 2000; Madhusudan *et al*., 2003). In such cases, a numerical method should be used, such as the Runge–Kutta method (Dormand and Prince, 1980; Butcher, 1995), the Differential Transformation Method (DTM) (Zhou, 1986), or the FEM (Bathe, 2006), since the differential equations become more complex.

The governing ODEs for geometrically exact beam theory with only bending deformation are widely available in literature. On the other hand, there is a scarcity of such equations when dealing with beams or columns that include axial and/or shear deformations under general loading conditions. In these cases, it is common to resort to discrete models, such as the FEM, to obtain numerical solutions. However, verifying the convergence of these results is not always possible.

Studies conducted by Huddleston (1972), Schmidt and Dadeppo (1972), Chaisomphob (1986), Goto *et al*. (1987, 1990), Sotiropoulou and Panayotounakos (2004), and Emam and Lacarbonara (2021) considered axial and/or shear deformations in prismatic members subjected solely to concentrated loads. However, the results reported in these studies were generally not tabulated, which significantly hinders accurate comparative analyses. Consequently, extracting results from graphs is insufficient to verify the convergence of a numerical method. Furthermore, in the few instances where results are presented in tables, they are often provided with limited accuracy, either due to mathematical approximations in the formulations or to the use of numerical methods with inadequate convergence tolerances.

Additionally, axial deformation influences both the value of the critical load and the equilibrium configuration of the member (Filipich and Rosales, 2000; Magnusson *et al*., 2001; Humer and Irschik, 2011). Therefore, its consideration is essential, particularly in post-buckling analyses, since neglecting it may lead to an overestimation of the load-carrying capacity. However, to the best of the authors' knowledge, there is no study in scientific literature based on a mathematical model that accounts for axial deformation in non-prismatic members subjected to either concentrated or uniformly distributed loads, where numerical results are tabulated with high accuracy.

In this context, the main objective of this article is to provide highly accurate tabulated results for certain problems involving prismatic and non-prismatic planar cantilever beams and columns that are axially deformable under large deflections. This aims to be useful for validating other numerical methods used to solve strongly nonlinear ODEs, particularly formulations based on the FEM.

In this study, a mathematical model is presented that considers large deflections but small strains, in which three ODEs are derived to govern the positions in the direction of the *x*-axis, *y*-axis, and about the *z*-axis in the deformed configuration of prismatic and non-prismatic planar beams or columns with axial deformation, subjected to concentrated and/or distributed loads.

In solving the problems presented in the numerical results, the MATLAB®solver **ode45** is used, based on the fourth- and fifth-order Runge–Kutta method of Dormand and Prince (1980), combined with the shooting method, where the influence of axial deformation is easily computed.

2. Governing differential equations

The governing ODEs used in this study are derived by introducing the basic assumptions of Euler–Bernoulli theory for slender beams and columns (i.e., plane sections normal to the undeformed member axis remain plane and normal to the deformed axis), a linear elastic material, and the assumption that there is no change in the geometry of the cross-sections after loading. Furthermore, it is assumed that the initially straight member is under large deflection and small strain, subjected to concentrated and distributed loads, with its geometric properties varying arbitrarily along the arc length s.

Let N, Q, and M be the axial force, shear force, and bending moment, respectively, acting at O, and $N + dN$, $Q + dQ$, and $M + dM$ be the axial force, shear force, and bending moment at P, a distance $(1 + \varepsilon_0)ds$ from point O (Figure 1), where ds denotes the infinitesimal arc length neglecting axial deformation. The angle between the tangent to the elastic curve at O and the x-axis is denoted by θ. Corresponding to the length $(1 + \varepsilon_0)ds$, the change in slope from O to P is $d\theta$, so the angle at P is $\theta + d\theta$. The variable q represents an arbitrarily varying inclined external force per unit length, so the force $q\ ds$ acts on the infinitesimal element in question. Thus, the following geometric relationships are valid:

$$\frac{dx}{ds} = (1 + \varepsilon_0)\cos\theta, \qquad \frac{dy}{ds} = (1 + \varepsilon_0)\sin\theta \quad (1)$$

in which ε_0 is the axial deformation at the neutral axis.

The constitutive relation is given by Hooke's law in the form:

$$\sigma_x = E\,\varepsilon_x \tag{2}$$

in which σ_x is the normal stress in the x-axis direction, and E is Young's modulus. The normal strain ε_x in a generic fiber at a distance y relative to the neutral axis is given by

$$\varepsilon_x = \varepsilon_0 - y\,\frac{d\theta}{ds} \tag{3}$$

in which $d\theta/ds$ is the curvature of the deformed longitudinal axis. Thus, from Eqs. (2) and (3), the axial force and the bending moment are defined as

$$N = \int_A \sigma_x dA = EA\varepsilon_0, \qquad M = \int_A -y\sigma_x dA = EI\frac{d\theta}{ds} \tag{4}$$

in which A is the cross-sectional area, and I is the second moment of area of the cross-section about the centroidal z-axis.

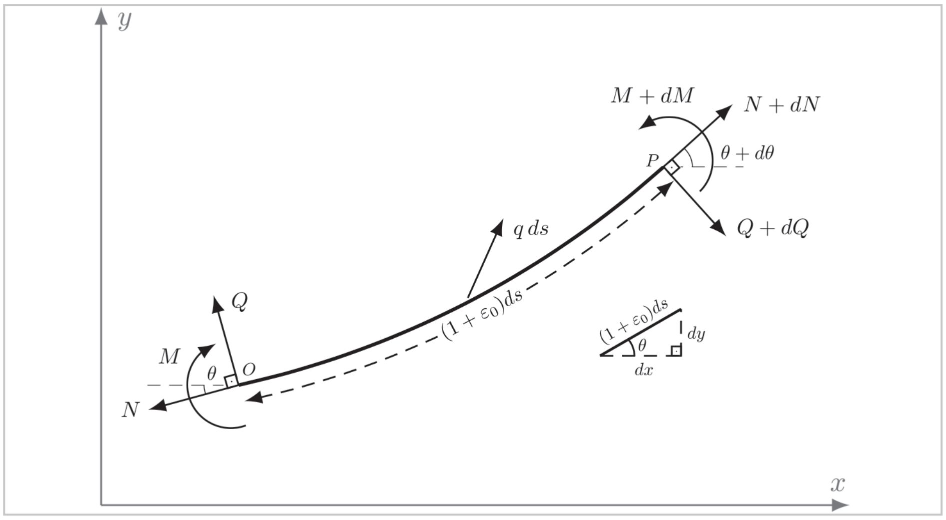

Figure 1 - The forces and bending moments acting on the deformed infinitesimal element.

The force equilibrium in the x- and y-axis directions at O, and the moment equilibrium about the z-axis at P of the infinitesimal element, provide the following equations:

$$\begin{aligned} -d\left(N\cos\theta\right) - d\left(Q\sin\theta\right) + q_x\,ds &= 0, \\ -d\left(N\sin\theta\right) + d\left(Q\cos\theta\right) + q_y\,ds &= 0, \\ -M + \left(M + dM\right) - Q\left(1+\varepsilon_0\right)ds &= 0 \end{aligned} \tag{5}$$

in which q_x and q_y are the components of q in the x- and y-directions, respectively. By integrating the first and second equations of Eq. (5) indefinitely, we obtain

$$\begin{aligned} -N\cos\theta - Q\sin\theta &= -\left(F_x + q_x s + c_1\right), \\ -N\sin\theta + Q\cos\theta &= -\left(F_y + q_y s + c_2\right) \end{aligned} \tag{6}$$

in which c_1 and c_2 are constants of integration, and F_x and F_y are concentrated loads acting in the x- and y-directions, respectively. The loads acting in the x-direction are considered positive if they cause tension in the member, whereas the loads acting in the y-direction are considered positive when acting upwards. Solving Eq. (6) for N and Q, we obtain

$$\begin{aligned} N &= \left(F_x + q_x s + c_1\right)\cos\theta + \left(F_y + q_y s + c_2\right)\sin\theta, \\ Q &= \left(F_x + q_x s + c_1\right)\sin\theta - \left(F_y + q_y s + c_2\right)\cos\theta \end{aligned} \tag{7}$$

The values of the constants c_1 and c_2 depend on the boundary conditions of the problem and the orientation of the coordinate system. A cantilever beam or column with the system positioned at the clamped end will have $c_1 = q_x(L - 2s)$ and $c_2 = q_y(L - 2s)$, where L is the length of the member in its undeformed configuration. On the other hand, for the same problem with the system positioned at the free end, $c_1 = c_2 = 0$.

From third equation of Eq. (5), we have

$$\frac{dM}{ds} - Q\left(1+\varepsilon_0\right) = 0 \tag{8}$$

Substituting Eq. (4) into Eq. (8), we obtain

$$\frac{d}{ds}\left(EI\,\frac{d\theta}{ds}\right) - Q\left(1+\frac{N}{EA}\right) = 0 \tag{9}$$

Similarly, by substituting Eq. (4) into Eq. (1), one obtains

$$\frac{dx}{ds} = \left(1+\frac{N}{EA}\right)\cos\theta \tag{10}$$

and

$$\frac{dy}{ds} = \left(1+\frac{N}{EA}\right)\sin\theta \tag{11}$$

in which EA is the axial rigidity, and EI is the flexural rigidity.

Therefore, the ODEs (9), (10), and (11) will provide the angular, longitudinal, and transverse positions, respectively, at an arbitrary point $s \in [0, L]$. It is noteworthy that by setting $EA \to \infty$, the same equations as those in the large deflection problem of inextensible beams or columns are obtained.

3. Numerical procedure

Consider a slender cantilever member (Figure 2) made of a material with Young's modulus E and a rectangular cross-section with a constant width b and a linearly varying height $h(x)$, where $h_A = \alpha h_B$ and $h_B = 1.5b$ represent the cross-sectional heights at points A and B, respectively, and α is the taper ratio. The cross-sectional area is given by $A(x) = bh(x)$, and the second moment of area is given by $I(x) = bh(x)^3/12$. The member AB, initially undeformed, has a length of $L = 20b$ and is subjected to concentrated forces F or uniformly distributed loads q in the x- or y-directions (Figure 3). Thus, after loading, the objective is to determine the positions x_A, y_A, and θ_A in the deformed configuration.

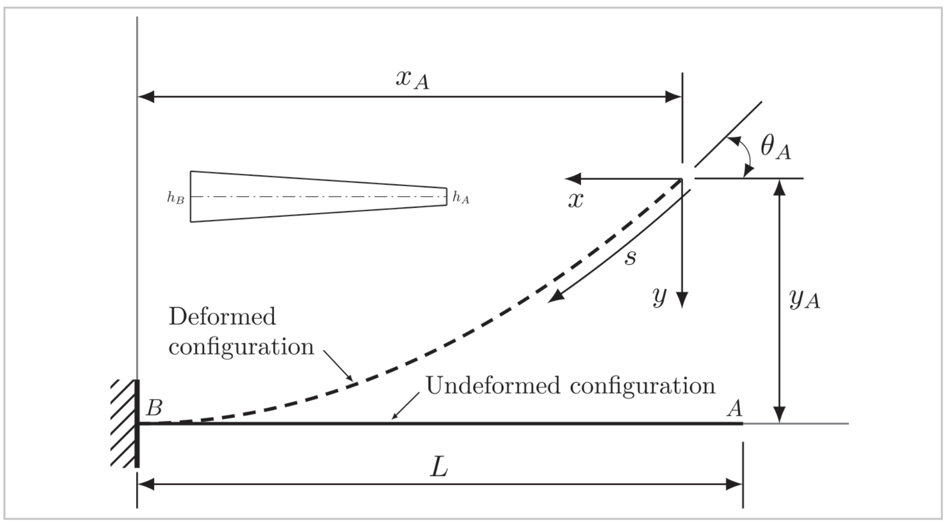

Figure 2 - Statement of the problem analyzed in the undeformed and deformed configurations.

However, when solving the nonlinear second-order two-point boundary value problem (Eq. 9) using the MATLAB® solver **ode45**, it is necessary to first rewrite it as an equivalent coupled system of two first-order ODEs. This procedure can be performed numerically with the help of the MATLAB® **odeToVectorField** function. Thus, Eqs. (9) to (11) will form a coupled system of four first-order ODEs, which, according to the problem shown in Figure 2, will be subject to the following boundary conditions:

$$x = 0, \quad y = 0, \quad \frac{d\theta}{ds} = 0 \quad \text{at} \quad s = 0, \qquad (12)$$
$$\theta = 0 \quad \text{at} \quad s = L$$

To satisfy the fourth condition in Eq. (12), the shooting method is used. However, when determining the load parameter for a specified rotation at the free end, this rotation must be imposed as an additional condition. Thus, the boundary conditions are given by:

$$x = 0, \quad y = 0, \quad \theta = \theta_A, \quad \frac{d\theta}{ds} = 0 \quad \text{at} \quad s = 0, \qquad (13)$$
$$\theta = 0 \quad \text{at} \quad s = L$$

The fifth condition in Eq. (13) is also satisfied using the shooting method by evaluating the rotation at the clamped end for a series of test loads. By identifying the load interval in which the rotation at the clamped end changes sign, the bisection method is applied within this interval to accurately determine the load at which the rotation becomes zero.

It is noteworthy that in the numerical analyses of the present study, the stopping criterion for satisfying the boundary conditions at the clamped end (Eqs. 12 and 13) was $\theta \leq |1.0 \times 10^{-10}|$. Additionally, the relative and absolute tolerances used in solving the ODEs were 2.22045×10^{-14} and 1.0×10^{-15}, respectively. However, in all numerical examples, the solutions stabilized and remained unchanged up to the sixth decimal place when the relative and absolute tolerances were set to $\leq 1.0 \times 10^{-6}$. Taper ratios smaller than 0.2 were not analyzed due to their theoretical and practical irrelevance in relation to the objectives of this study.

4. Numerical results

Figure 3 below presents the five load cases analyzed for the problem shown in Figure 2.

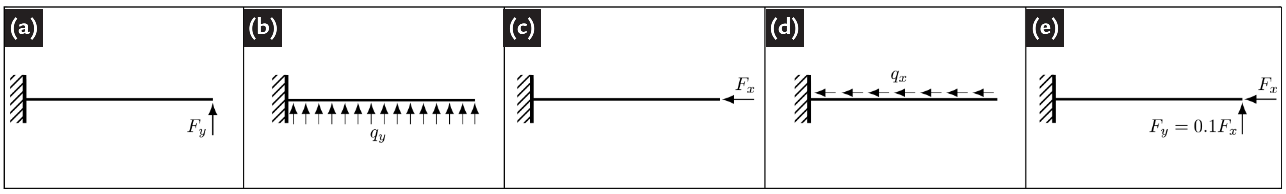

Figure 3 - Load cases analyzed for the problem in Figure 2.

4.1 Cantilever beam with a concentrated transverse load at the free end

In this problem, the geometrically nonlinear behavior of a cantilever beam subjected to a concentrated transverse load at the free end was evaluated (Figure 3a). Thus, dimensionless free-end positions were obtained for various values of taper ratio α and load parameter $F_yL^2/(EI_B)$.

Table 1 presents load parameter $F_yL^2/(EI_B)$ and dimensionless free-end positions x_A/L and y_A/L, for various values of α and a free-end rotation of θ_A = 80°, neglecting axial deformation. To compare the results, the values reported in Rao, B. N. and Rao, G. V. (1988b) are also included in this table. It is also noteworthy that for α = 1.0, an analytical solution in terms of elliptic integrals available in Timoshenko and Gere (1972) is provided. However, the integrals are evaluated using the MATLAB® **int** function. It can be observed in this table that there is good agreement between the values obtained from the present numerical analysis and those in Timoshenko and Gere (1972) and Rao, B. N. and Rao, G. V. (1988b).

Table 1 - Comparison of load parameter and dimensionless free-end positions of the cantilever beam, neglecting axial deformation, for various values of α and θ_A = 80°, under a concentrated transverse load.

Solution	α	$F_yL^2/(EI_B)$	x_A / L	y_A / L
Present analysis	0.2	1.44464	0.70695	0.57043
	0.4	3.08360	0.60739	0.67789
	0.6	4.85308	0.54821	0.73373
	0.8	6.72407	0.50718	0.76948
	1.0	8.67877	0.47639	0.79485
Numerical (Rao, B. N. and Rao, G. V., 1988b)	0.2	1.44460	0.71029	0.57043
	0.4	3.08360	0.61072	0.67789
	0.6	4.85310	0.55154	0.73373
	0.8	6.72410	0.51052	0.76948
	1.0	8.67880	-	-
Analytical (Timoshenko and Gere, 1972)	1.0	8.67877	0.47639	0.79485

Table 2 presents dimensionless free-end positions x_A/L, y_A/L, and θ_A for various values of α and $F_yL^2/(EI_B\alpha)$ from the present analysis, considering axial deformation.

Table 2 - Dimensionless free-end positions of the cantilever beam with axial deformation, for various values of α and $F_yL^2/(EI_B\alpha)$, under a concentrated transverse load.

$F_yL^2/(EI_B\alpha)$	α = 0.2			α = 0.6			α = 1.0		
	x_A/L	y_A/L	θ_A	x_A/L	y_A/L	θ_A	x_A/L	y_A/L	θ_A
1.0	0.973942	0.178577	0.467007	0.953825	0.264216	0.463466	0.943682	0.301813	0.461421
2.0	0.920333	0.308624	0.804569	0.865594	0.439313	0.790147	0.839617	0.493875	0.782034
3.0	0.866010	0.395957	1.024051	0.783361	0.544413	0.999974	0.745921	0.604078	0.986513
4.0	0.818444	0.457033	1.168561	0.716232	0.610985	1.138699	0.671448	0.671207	1.121895
5.0	0.777909	0.502260	1.267192	0.662235	0.656367	1.234674	0.612795	0.715452	1.216135
6.0	0.743255	0.537405	1.336846	0.618264	0.689308	1.303730	0.565863	0.746648	1.284540
7.0	0.713312	0.565754	1.387456	0.581822	0.714439	1.355001	0.527549	0.769862	1.335851
8.0	0.687134	0.589288	1.425097	0.551098	0.734374	1.394033	0.495673	0.787892	1.375351
9.0	0.663994	0.609264	1.453636	0.524793	0.750681	1.424354	0.468703	0.802383	1.406398
10.0	0.643338	0.626525	1.475629	0.501968	0.764351	1.448306	0.445550	0.814357	1.431221

Figure 4 shows the relative error of dimensionless free-end positions when axial deformation is neglected, for various values of α and $F_yL^2/(EI_B\alpha)$ = 10.0. The relative error increases with α, reaching a maximum at α = 1.0, with values of 0.12%, 0.46%, and 0.07% for x_A/L, y_A/L, and θ_A, respectively.

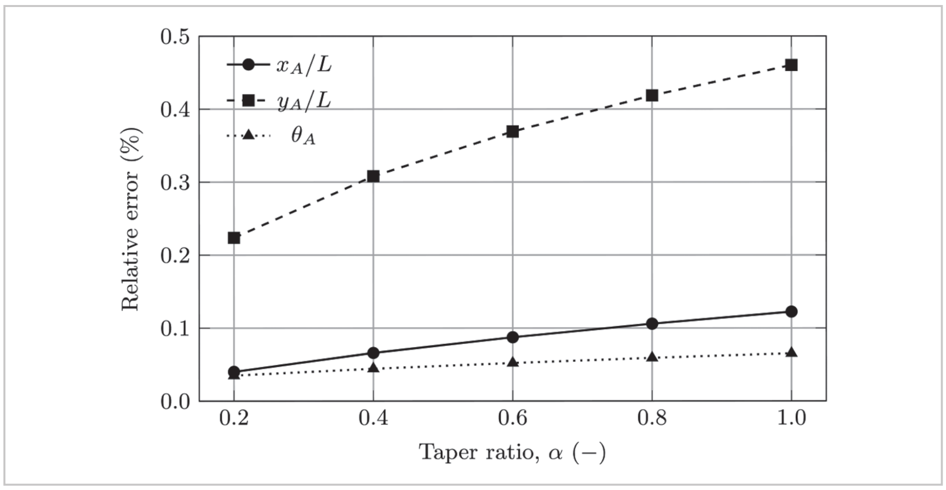

Figure 4 - Relative error of dimensionless free-end positions of the cantilever beam, neglecting axial deformation, for various values of α and $F_yL^2/(EI_B\alpha)$ = 10.0, under a concentrated transverse load.

4.2 Cantilever beam with a uniformly distributed transverse load

In this problem, the geometrically nonlinear behavior of a cantilever beam subjected to a uniformly distributed transverse load was evaluated (Figure 3b). Thus, dimensionless free-end positions were obtained for various values of taper ratio α and load parameter $q_yL^3/(EI_B\alpha)$.

Table 3 presents dimensionless free-end positions x_A/L, y_A/L, and θ_A for α = 1.0 and $q_yL^3/(EI_B\alpha)$ = 32.0, neglecting axial deformation. For comparison purposes, the value of the rotation reported in Rao, B. N. and Rao, G. V. (1989) is also included in this table, showing good agreement between the two solutions.

Table 3 - Comparison of dimensionless free-end positions of the cantilever beam, neglecting axial deformation, for α = 1.0 and $q_yL^3/(EI_B\alpha)$ = 32.0, under a uniformly distributed transverse load.

Solution	x_A/L	y_A/L	θ_A
Present analysis	0.32849	0.87846	1.46136
Numerical (Rao, B. N. and Rao, G. V., 1989)	-	-	1.46136

Table 4 presents dimensionless free-end positions x_A/L, y_A/L, and θ_A for various values of α and $q_yL^3/(EI_B\alpha)$ from the present analysis, considering axial deformation.

Table 4 - Dimensionless free-end positions of the cantilever beam with axial deformation, for various values of α and $q_yL^3/(EI_B\alpha)$, under a uniformly distributed transverse load.

$q_yL^3/(EI_B\alpha)$	α = 0.2			α = 0.6			α = 1.0		
	x_A/L	y_A/L	θ_A	x_A/L	y_A/L	θ_A	x_A/L	y_A/L	θ_A
1.0	0.998132	0.053147	0.095351	0.994165	0.098933	0.143547	0.991269	0.123478	0.165120
2.0	0.992634	0.105366	0.189278	0.977560	0.193117	0.281697	0.966973	0.238552	0.321626
3.0	0.983813	0.155827	0.280490	0.952490	0.279038	0.410311	0.931664	0.339780	0.463633
4.0	0.972119	0.203864	0.367934	0.921786	0.354934	0.527082	0.890333	0.425420	0.588771
5.0	0.958082	0.249019	0.450847	0.888048	0.420563	0.631352	0.846937	0.496326	0.697287
6.0	0.942251	0.291031	0.528756	0.853279	0.476640	0.723571	0.804049	0.554525	0.790772
7.0	0.925140	0.329813	0.601445	0.818840	0.524314	0.804771	0.763110	0.602274	0.871254
8.0	0.907203	0.365413	0.668907	0.785572	0.564831	0.876198	0.724803	0.641621	0.940726
9.0	0.888820	0.397968	0.731279	0.753937	0.599360	0.939102	0.689359	0.674272	1.000954
10.0	0.870295	0.427675	0.788801	0.724151	0.628919	0.994633	0.656758	0.701590	1.053433
11.0	0.851860	0.454756	0.841768	0.696273	0.654363	1.043808	0.626854	0.724647	1.099400
12.0	0.833691	0.479444	0.890505	0.670270	0.676399	1.087503	0.599444	0.744275	1.139872
13.0	0.815915	0.501967	0.935340	0.646057	0.695603	1.126467	0.574306	0.761128	1.175683
14.0	0.798618	0.522542	0.976599	0.623523	0.712442	1.161332	0.551224	0.775714	1.207515
15.0	0.781856	0.541369	1.014589	0.602549	0.727297	1.192636	0.529992	0.788437	1.235934

Figure 5 shows the relative error of dimensionless free-end positions when axial deformation is neglected, for various values of α and $q_yL^3/(EI_B\alpha)$ = 15.0. The relative error increases with α, reaching a maximum at α = 1.0, with values of 0.08%, 0.30%, and 0.09% for x_A/L, y_A/L, and θ_A, respectively.

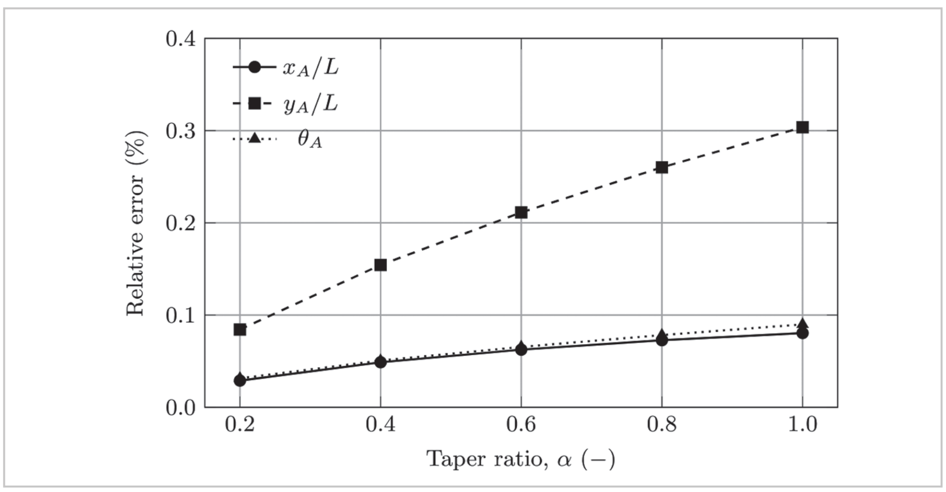

Figure 5 - Relative error of dimensionless free-end positions of the cantilever beam, neglecting axial deformation, for various values of α and $q_yL^3/(EI_B\alpha)$ = 15.0, under a uniformly distributed transverse load.

4.3 Cantilever column with a concentrated axial load at the free end

In this problem, the buckling and post-buckling behavior of a cantilever column subjected to a concentrated compressive axial load at the free end was evaluated (Figure 3c). Thus, load parameter and dimensionless positions of the free end were obtained for various values of taper ratio α and free-end rotation θ_A.

Table 5 presents load parameter $F_xL^2/(EI_B)$ and dimensionless free-end positions x_A/L and y_A/L for α = 1.0 and θ_A = 160°, neglecting axial deformation. For comparison purposes, the values reported in Lee (2001) are also included in this table. It is further noted that an analytical solution in terms of elliptic integrals, available in Timoshenko and Gere (1961), is provided. However, to increase the accuracy of the results, they were recalculated with the help of the MATLAB® **int** function. It can be observed in this table that there is good agreement between the values obtained from the present numerical analysis and those in Timoshenko and Gere (1961) and Lee (2001).

Table 5 - Comparison of load parameter and dimensionless free-end positions of the cantilever column, neglecting axial deformation, for α = 1.0 and θ_A = 160°, under a concentrated axial load.

Solution	$F_xL^2/(EI_B)$	x_A/L	y_A/L
Present analysis	9.94384	-0.34032	0.62460
Numerical (Lee, 2001)	9.94280	-0.34040	0.62470
Analytical (Timoshenko and Gere, 1961)	9.94384	-0.34032	0.62460

Table 6 presents load parameter $F_xL^2/(EI_B)$ and dimensionless free-end positions x_A/L and y_A/L for various values of α and θ_A from the present analysis, considering axial deformation.

Table 6 - Load parameter and dimensionless free-end positions of the cantilever column with axial deformation, for various values of α and θ_A, under a concentrated axial load.

θ_A (deg.)	α = 0.2			α = 0.6			α = 1.0		
	$F_xL^2/(EI_B)$	x_A/L	y_A/L	$F_xL^2/(EI_B)$	x_A/L	y_A/L	$F_xL^2/(EI_B)$	x_A/L	y_A/L
0	0.597396	0.999437	0	1.570728	0.999060	0	2.470262	0.998842	0
20	0.604710	0.988477	0.105871	1.593100	0.975669	0.183842	2.508207	0.968625	0.219165
40	0.627468	0.955856	0.208073	1.663046	0.906893	0.356120	2.627149	0.880241	0.421797
60	0.668356	0.902258	0.303181	1.789958	0.796760	0.506042	2.844107	0.740256	0.592666
80	0.732832	0.828493	0.388210	1.993130	0.651438	0.624254	3.194297	0.558832	0.718984
100	0.831362	0.734879	0.460734	2.310160	0.478367	0.703241	3.747052	0.348550	0.791191
120	0.985360	0.619949	0.518806	2.819383	0.284823	0.737245	4.648652	0.122674	0.803117
140	1.246622	0.477093	0.560315	3.713889	0.075014	0.720926	6.264745	-0.107786	0.750740
160	1.795686	0.281117	0.579617	5.679914	-0.159679	0.642686	9.914367	-0.342359	0.625487
176	3.494724	-0.024663	0.548585	12.123436	-0.435095	0.482222	22.309836	-0.583709	0.423170

Figure 6 shows the relative error of load parameter and dimensionless free-end positions when axial deformation is neglected, for various values of α and θ_A = 176°. For $F_xL^2/(EI_B)$ and y_A/L, the relative error increases with α, reaching a maximum at α = 1.0, with values of 0.82% and 0.41%, respectively. However, for x_A/L, the relative error reaches a maximum of 2.97% at α = 0.2, then decreases rapidly to 0.80% at α = 0.4, followed by a gradual increase to 1.11% at α = 1.0.

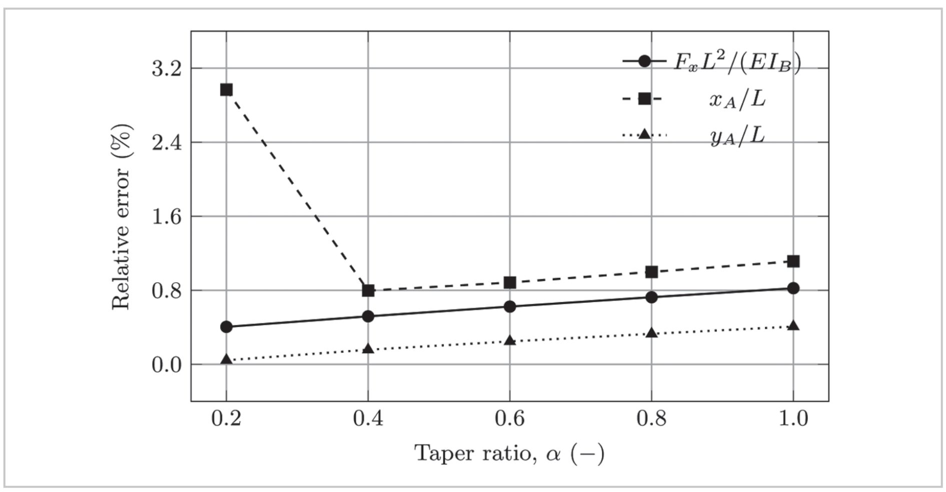

Figure 6 - Relative error of load parameter and dimensionless free-end positions of the cantilever column, neglecting axial deformation, for various values of α and θ_A = 176°, under a concentrated axial load.

4.4 Cantilever column with a uniformly distributed axial load

In this problem, the buckling and post-buckling behavior of a cantilever column subjected to a uniformly distributed compressive axial load was evaluated (Figure 3d). Thus, load parameter and dimensionless positions of the free end were obtained for various values of taper ratio α and free-end rotation θ_A.

Table 7 presents load parameter $q_xL^3/(EI_B)$ and dimensionless free-end positions x_A/L and y_A/L for α = 1.0 and θ_A = 160°, neglecting axial deformation. To compare the results, the values reported in Rao, B. N. and Rao, G. V. (1988a) are also included in this table, showing good agreement between the two solutions.

Table 7 - Comparison of load parameter and dimensionless free-end positions of the cantilever column, neglecting axial deformation, for α = 1.0 and θ_A = 160°, under a uniformly distributed axial load.

Solution	$q_x L^3/(EI_B)$	x_A/L	y_A/L
Present analysis	28.13278	-0.50816	0.56570
Numerical (Rao, B. N. and Rao, G. V., 1988a)	28.13280	-0.50480	0.56670

Table 8 presents load parameter $q_x L^3/(EI_B)$ and dimensionless free-end positions x_A/L and y_A/L for various values of α and θ_A from the present analysis, considering axial deformation.

Table 8 - Load parameter and dimensionless free-end positions of the cantilever column with axial deformation, for various values of α and θ_A, under a uniformly distributed axial load.

θ_A (deg.)	α = 0.2			α = 0.6			α = 1.0		
	$q_x L^3/(EI_B)$	x_A/L	y_A/L	$q_x L^3/(EI_B)$	x_A/L	y_A/L	$q_x L^3/(EI_B)$	x_A/L	y_A/L
0	3.395388	0.998811	0	5.787334	0.998415	0	7.851036	0.998160	0
20	3.428710	0.978653	0.162696	5.860563	0.967109	0.221669	7.960660	0.961543	0.246858
40	3.532281	0.918977	0.316764	6.088988	0.875477	0.426289	8.303383	0.854796	0.472438
60	3.718030	0.822084	0.453932	6.501566	0.730143	0.598075	8.925228	0.686918	0.657291
80	4.010304	0.691468	0.566565	7.157587	0.541414	0.723606	9.920828	0.471873	0.785409
100	4.456153	0.531232	0.647744	8.172105	0.322171	0.792592	11.474898	0.227105	0.845383
120	5.152624	0.345015	0.690919	9.783697	0.086259	0.798017	13.973091	-0.028514	0.830824
140	6.336076	0.133478	0.688363	12.577286	-0.154160	0.734922	18.367989	-0.277633	0.739326
160	8.832933	-0.115217	0.624277	18.617142	-0.395865	0.593962	28.048663	-0.511072	0.566491
176	16.566836	-0.413632	0.471704	37.949068	-0.632169	0.378291	59.768897	-0.717592	0.331209

Figure 7 shows the relative error of load parameter and dimensionless free-end positions when axial deformation is neglected, for various values of α and θ_A = 176°. The relative error increases with α, reaching a maximum at α = 1.0, with values of 0.99%, 1.21%, and 0.50% for $q_x L^3/(EI_B)$, x_A/L, and y_A/L, respectively.

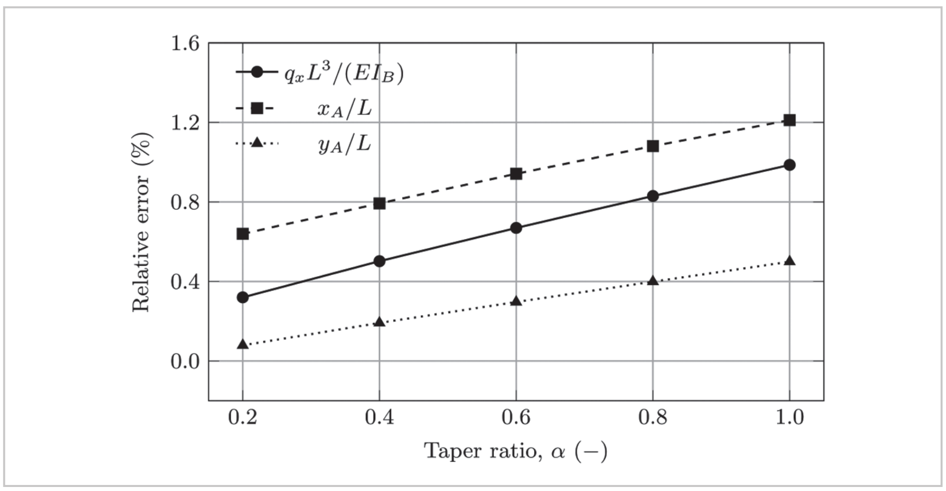

Figure 7 - Relative error of load parameter and dimensionless free-end positions of the cantilever column, neglecting axial deformation, for various values of α and θ_A = 176°, under a uniformly distributed axial load.

4.5 Cantilever column with combined concentrated axial and transverse loads at the free end

In this problem, the geometrically nonlinear behavior of a cantilever column subjected to combined concentrated axial and transverse loads at the free end was evaluated (Figure 3e). Thus, dimensionless free-end positions were obtained for various values of taper ratio α and load parameter $F_x L^2/(EI_B \alpha)$.

Table 9 presents dimensionless free-end positions $x_A/L, y_A/L$, and θ_A for various values of α and $F_xL^2/(EI_B\alpha)$ from the present analysis, considering axial deformation.

Table 9 - Dimensionless free-end positions of the cantilever column with axial deformation, for various values of α and $F_xL^2/(EI_B\alpha)$, under combined concentrated axial and transverse loads.

$F_xL^2/(EI_B\alpha)$	α = 0.2			α = 0.6			α = 1.0		
	x_A/L	y_A/L	θ_A	x_A/L	y_A/L	θ_A	x_A/L	y_A/L	θ_A
1.0	0.999153	0.027885	0.077775	0.998243	0.046137	0.082185	0.997668	0.055457	0.084744
2.0	0.989901	0.103802	0.312339	0.968360	0.212712	0.395495	0.947862	0.284584	0.451897
3.0	0.889755	0.326775	1.087416	0.693334	0.599412	1.292305	0.574271	0.713018	1.362529
4.0	0.721027	0.478015	1.754535	0.415606	0.724690	1.845668	0.264116	0.806353	1.867272
5.0	0.589001	0.541078	2.131248	0.233352	0.744807	2.159986	0.071154	0.801944	2.157811
6.0	0.487205	0.570923	2.367603	0.107152	0.735472	2.362978	-0.057755	0.774347	2.348154
7.0	0.405468	0.586042	2.527439	0.014174	0.717285	2.504318	-0.149895	0.742282	2.482503
8.0	0.337567	0.593625	2.640865	-0.057743	0.696948	2.607587	-0.219304	0.711168	2.581989
9.0	0.279699	0.596957	2.724103	-0.115488	0.676854	2.685616	-0.273760	0.682546	2.658176
10.0	0.229421	0.597724	2.786728	-0.163218	0.657852	2.746061	-0.317875	0.656688	2.717995

Figure 8 shows the relative error of dimensionless free-end positions when axial deformation is neglected, for various values of α and $F_xL^2/(EI_B\alpha)$ = 10.0. For y_A/L and θ_A, the relative error increases with α, reaching a maximum at α = 1.0, with values of 0.06% and 0.06%, respectively. However, for x_A/L, the relative error reaches a maximum of 7.60% at α = 0.4, then decreases rapidly to 1.50% at α = 0.6, and continues to decrease to 1.02% at α = 1.0.

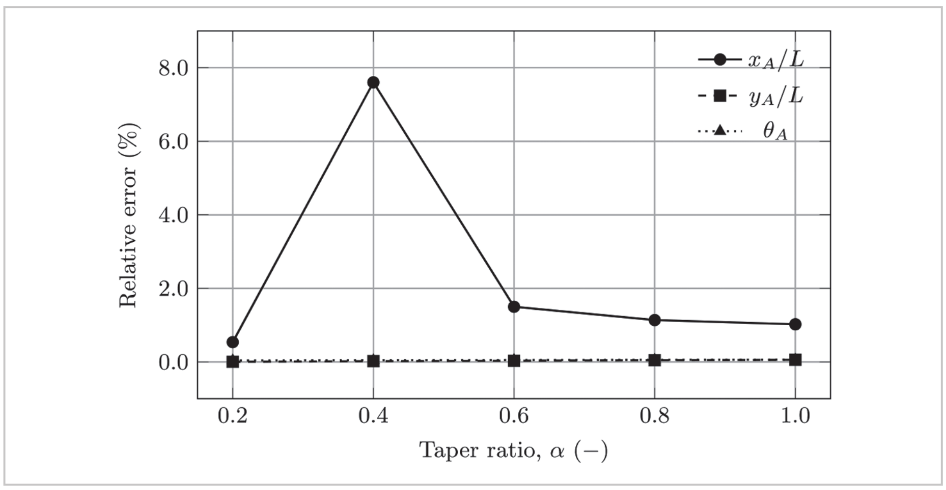

Figure 8 - Relative error of dimensionless free-end positions of the cantilever column, neglecting axial deformation, for various values of α and $F_xL^2/(EI_B\alpha)$ = 10.0, under combined concentrated axial and transverse loads.

5. Conclusions

An analysis of large deflections in certain beam and column problems, considering the influence of axial deformation for a specific slenderness ratio, was conducted. Numerical solutions for various taper ratios, load parameters, and free-end rotations were obtained and compared with numerical and analytical results available in literature, showing good agreement. To facilitate the comparison of numerical data in potential validations of other methods and formulations, the highly accurate results are provided in tabular form, up to six decimal places. As shown by the results, the influence of axial deformation is negligible in cases where bending is predominant (e.g., members subjected to transverse loads). However, in cases where the loading is predominantly axial (e.g., members subjected to axial loads or to both axial and transverse loads), the influence of axial deformation can be significant, depending on the taper ratio. Although other combined load cases were not analyzed, the proposed mathematical model can be applied to general load cases and boundary conditions, involving slender planar members with axial deformability.

Acknowledgements

The authors acknowledge the financial support provided by the Brazilian research agencies CNPq (Conselho Nacional de Desenvolvimento Científico e Tecnológico) under grant number 302119/2022-1 and FAPEMIG (Fundação de Amparo à Pesquisa do Estado de Minas Gerais) under grant number 23072.229666/2022-13.

References

BAKER, G. On the large deflections of non-prismatic cantilevers with a finite depth. ***Computers & Structures,*** v. 46, n. 2, p. 365-370, 1993.

BARTEN, H. J. On the deflection of a cantilever beam. ***Quarterly of Applied Mathematics,*** v. 2, n. 2, p. 168-171, 1944.

BATHE, K. J. ***Finite element procedures.*** Klaus-Jurgen Bathe, 2006.

BICKLEY, W. G. L. The heavy elastica. ***The London, Edinburgh, and Dublin Philosophical Magazine and Journal of Science,*** v. 17, n. 113, p. 603-622, 1934.

BISSHOPP, K. E.; DRUCKER, D. C. Large deflection of cantilever beams. ***Quarterly of Applied Mathematics,*** v. 3, n. 3, p. 272-275, 1945.

BUTCHER, J. C. On fifth order Runge-Kutta methods. ***BIT Numerical Mathematics,*** v. 35, n. 2, p. 202-209, 1995.

CHAISOMPHOB, T. *et al*. An elastic finite displacement analysis of plane beams with and without shear deformation. ***Doboku Gakkai Ronbunshu,*** v. 1986, n. 368, p. 169-177, 1986.

CONWAY, H. D. The large deflection of simply supported beams. ***The London, Edinburgh, and Dublin Philosophical Magazine and Journal of Science,*** v. 7, n. 38, p. 905-911, 1947.

DORMAND, J. R.; PRINCE, P. J. A family of embedded Runge-Kutta formulae. ***Journal of Computational and Applied Mathematics,*** v. 6, n. 1, p. 19-26, 1980.

EMAM, S.; LACARBONARA, W. Buckling and postbuckling of extensible, shear-deformable beams: some exact solutions and new insights. ***International Journal of Non-Linear Mechanics,*** v. 129, p. 103667, 2021.

FILIPICH, C. P.; ROSALES, M. B. A further study on the postbuckling of extensible elastic rods. ***International Journal of Non-Linear Mechanics,*** v. 35, n. 6, p. 997-1022, 2000.

FRISCH-FAY, R. The analysis of a vertical and a horizontal cantilever under a uniformly distributed load. ***Journal of the Franklin Institute,*** v. 271, n. 3, p. 192-199, 1961.

FRISCH-FAY, R. Large deflections of a cantilever under two concentrated loads. ***Journal of Applied Mechanics,*** v. 29, n. 1, p. 200-201, 1962a.

FRISCH-FAY, R. ***Flexible bars.*** Butterworths, London, 1962b.

GOTO, Y. *et al*. Elliptic integral solutions for extensional elastica with constant initial curvature. ***Doboku Gakkai Ronbunshu,*** v. 1987, n. 386, p. 83-93, 1987.

GOTO, Y. *et al*. Elliptic integral solutions of plane elastica with axial and shear deformations. ***International Journal of Solids and Structures,*** v. 26, n. 4, p. 375-390, 1990.

HOLDEN, J. T. On the finite deflections of thin beams. ***International Journal of Solids and Structures,*** v. 8, n. 8, p. 1051-1055, 1972.

HUDDLESTON, J. V. Effect of shear deformation on the elastica with axial strain. ***International Journal for Numerical Methods in Engineering,*** v. 4, n. 3, p. 433-444, 1972.

HUMER, A.; IRSCHIK, H. Large deformation and stability of an extensible elastica with an unknown length. ***International Journal of Solids and Structures,*** v. 48, n. 9, p. 1301-1310, 2011.

HUMMEL, F. H.; MORTON, W. B. On the large bending of thin flexible strips and the measurement of their elasticity. ***The London, Edinburgh, and Dublin Philosophical Magazine and Journal of Science,*** v. 4, n. 21, p. 348-357, 1927.

LEE, B. K.; OH, S. J. Elastica and buckling load of simple tapered columns with constant volume. ***International Journal of Solids and Structures,*** v. 37, n. 18, p. 2507-2518, 2000.

LEE, K. Post-buckling of uniform cantilever column under a combined load. ***International Journal of Non-Linear Mechanics,*** v. 36, n. 5, p. 813-816, 2001.

MADHUSUDAN, B. P. *et al*. Post-buckling of cantilever columns having variable cross-section under a combined load. ***International Journal of Non-Linear Mechanics,*** v. 38, n. 10, p. 1513-1522, 2003.

MAGNUSSON, A. *et al*. Behaviour of the extensible elastica solution. ***International Journal of Solids and Structures,*** v. 38, n. 46-47, p. 8441-8457, 2001.

MATTIASSON, K. Numerical results from large deflection beam and frame problems analysed by means of elliptic integrals. ***International Journal for Numerical Methods in Engineering,*** v. 17, n. 1, p. 145-153, 1981.

RAO, B. N.; RAO, G. V. Large deflection analysis of a nonlinear elastic column under uniformly distributed axial load. ***Forschung im Ingenieurwesen A,*** v. 54, n. 5, p. 153-160, 1988a.

RAO, B. N.; RAO, G. V. Large deflections of a nonuniform cantilever beam with end rotational load. ***Forschung im Ingenieurwesen A,*** v. 54, n. 1, p. 24-26, 1988b.

RAO, B. N.; RAO, G. V. Large deflections of a cantilever beam subjected to a rotational distributed loading. ***Forschung im Ingenieurwesen A,*** v. 55, p. 116-120, 1989.

RAO, G. V.; RAJU, P. C. Post-buckling of uniform cantilever columns - galerkin finite element solution. ***Engineering***

Fracture Mechanics, v. 9, n. 1, p. 1-4, 1977.
ROHDE, F. V. Large deflections of a cantilever beam with uniformly distributed load. ***Quarterly of Applied Mathematics,*** v. 11, n. 3, p. 337-338, 1953.
SCHMIDT, R.; DADEPPO, D. A. Large deflections of heavy cantilever beams and columns. ***Quarterly of Applied Mathematics,*** v. 28, n. 3, p. 441-444, 1970.
SCHMIDT, R.; DADEPPO, D. A. Nonlinear theory of arches and beams with shear deformation. ***Journal of Applied Mechanics,*** v. 39, n. 4, p. 1144-1146, 1972.
SEIDE, P. Large deflections of a simply supported beam subjected to moment at one end. ***Journal of Applied Mechanics,*** v. 51, n. 3, p. 519-525, 1984.
SOTIROPOULOU, A. B.; PANAYOTOUNAKOS, D. E. Exact parametric analytic solutions of the elastica ODEs for bars including effects of the transverse deformation. ***International Journal of Non-Linear Mechanics,*** v. 39, n. 10, p. 1555-1570, 2004.
TIMOSHENKO, S. P.; GERE, J. M. ***Theory of elastic stability.*** McGraw-Hill Book Co. Inc., New York, 1961.
TIMOSHENKO, S. P.; GERE, J. M. ***Mechanics of materials.*** Van Nordstrand Reinhold Company. New York, 1972.
WANG, C. M. *et al*. Large deflections of an end supported beam subjected to a point load. ***International Journal of Non-Linear Mechanics,*** v. 32, n. 1, p. 63-72, 1997.
WANG, C. Y. Large deformations of a heavy cantilever. ***Quarterly of Applied Mathematics,*** v. 39, n. 2, p. 261-273, 1981.
WANG, C. Y. Buckling and postbuckling of heavy columns. ***Journal of Engineering Mechanics,*** v. 113, n. 8, p. 1229-1233, 1987.
ZHOU, J. K. Differential transformation and its applications for electrical circuits. ***Huazhong University Press, Wuhan China (In Chinese),*** v. 2, p. 413-420, 1986.

Received: 20 June 2025 - Accepted: 10 November 2025.

Authors' contributions

Aleff Gonçalves Quintino (Corresponding author): *conceptualization (lead), data curation (lead), formal analysis (lead), investigation (lead), methodology (lead), software (lead): validation (lead), visualization (equal), writing - original draft (lead), writing - review & editing (lead);* **Marcelo Greco:** *funding acquisition (lead), project administration (lead), resources (lead), supervision (lead), validation (supporting), visualization (equal).*

Funding information

This research was funded by CNPq (Conselho Nacional de Desenvolvimento Científico e Tecnológico) under grant number 302119/2022-1 and FAPEMIG (Fundação de Amparo à Pesquisa do Estado de Minas Gerais) under grant number 23072.229666/2022-13.

Conflict of interests

The authors declare that there is no conflict of interest.

Data availability

The data supporting the findings of this study will be made available from the corresponding author, Aleff Gonçalves Quintino, upon reasonable request, at the following email address: aleff.quintino@gmail.com.

Associate Editor

Diogo Rodrigo Ferreira Ribeiro